

## The Use of Sentinel-2A Images to Estimate Potential Flood Risk With A Multi-Index Approach in The Mempawah Watershed

Ajun Purwanto\*, Paiman, Agus Sudiro

Department of Geography Education, IKIP PGRI Pontianak, Jl. Ampera No.88, Sungai Jawi, Kota Pontianak, West Kalimantan, Indonesia

\*Corresponding author, Email address : [ajunpurwanto@ikipgriptk.co.id](mailto:ajunpurwanto@ikipgriptk.co.id)

### ARTICLE INFO

Received :  
13 January 2023

Revised :  
19 April 2023

Accepted :  
26 April 2023

Published :  
30 April 2023

### ABSTRACT

Natural disasters in Indonesia have become an annual cycle, an example is flooding. This study aims to determine the flood risk potential in the Mempawah watershed and the places likely to be flooded. The method used was a survey and interpretation of secondary data from topographic maps, Sentinel-2A images, and Digital Elevation Model images. Furthermore, the secondary data analysis used includes the Standardized Precipitation Index (SPI), Normalized Difference Vegetation Index (NDVI), Normalized Difference Water Index (NDWI), Soil Adjusted Vegetation Index (SAVI), and Inverse Distance Weighted (IDW). The result showed that the Mempawah watershed has high, medium, and low flood risk potential. Areas with high flood potential have an area of 1,511,967 ha, those with medium potential were 2,606,778 ha, and the places with low potential were 12,644,034 ha. The changes in class user's accuracy results reached 90.909%, while those with no change were 83.333%. It was also discovered that when the satellite analysis was > 70%, it was regarded as good. This means that the accuracy of the interpretation results and flood change detection approach was also good.

**Keywords :** Sentinel-2A; Estimation Potential; Flood Risk; Watershed

### INTRODUCTION

Natural disasters are phenomena that occur at any time and anywhere. In Indonesia, this occurrence is an annual cycle and needs to be anticipated and managed. One of the natural disasters that often occur yearly is flooding and it has affected many areas in different regions, caused damage, and even results in death (Caballero et al., 2019; Faizana et al., 2015; Laurenz et al., 2019). Moreover, many people living on riverbanks and flood-prone places do not care about these conditions.

The hydrological cycles of the nearby watershed are significantly impacted by land-use change. Many factors cause flooding, including climate, land structure, slope, humans (Curebal et al., 2016), and also changes in land use (Ali et al., 2020; Caruso, 2017; Curebal et al., 2016; Dano et al., 2019; Rincón et al., 2018). Floods are also caused by conditions of complex hydrology, geology

and geomorphology, illegal logging (Sholihah et al., 2020), urbanization, and a substantially unbalanced environment (Mukherjee & Singh, 2020; Komolafe et al., 2020; Skilodimou et al., 2019). Many studies have been carried out to evaluate the effects of changes in surface land use on flows (Abdelkarim, et al., 2019; Brath et al., 2006; Mao & Cherkauer, 2009; Sheng & Wilson, 2009).

One of the contributing variables for land use and land cover (LULC) is the efforts of meeting human needs, such as the construction of housing facilities, industry, agriculture, mining, and other infrastructure (Abdelkarim et al., 2019; Rawat et al., 2013), to spur sustainable economic growth in the area. Due to their effect on natural ecosystems, land-use change detection has become a concern for environmentalists, conservationists, and land-use planners (Halmy et al., 2015).

In addition, changes in land use are risky and often become a serious problem when not managed properly. Example of the problems that arise is flooding, which served as a significant challenge for several cities in developed and developing countries (Abdelkarim et al., 2019). Therefore, the effective utilization of data on flood risk maps and their frequency is needed when designing water resources and urban planning in order to assess residents and infrastructure's vulnerability to floods (Fernández & Lutz, 2010).

Since July 2021, heavy rainfall has been experienced in several areas of West Kalimantan, such as Kapuas Hulu, Melawi, Landak, and Ketapang. The heavy rains and high waves, accompanied by strong winds triggered flooding. An example of the recent floods in September occurred in Mempawah Regency, West Kalimantan, of which six sub-districts were affected for one week. In addition, the number of houses affected was 674, which includes 7,885 families and 26,245 people (Muhari, 2021).

It is essential to remember that uncontrolled land-use shift in upstream areas often triggers flooding, particularly due to heavy rainfall. According to (Huong & Pathirana, 2013), increased urban activity in flooded areas usually enhance peak period, lessen peak discharge, and boost surface runoff. This makes conclude that a improved comprehension and evaluation of land-use change directly impacted watershed hydrological processes (Diakakis et al., 2020).

Consequently, similar flood cases have to be prevented in the coming years. At times, it is possible to predict flood-prone places, which eventually reduces the loss of property and even lives. Employed remote sensing and GIS as practical and effective tools for estimating and predicting flood disasters (Purwanto et al., 2022; Zhu & Woodcock, 2014). Some researcher said utilized a high-accuracy Sentinel-2 Imagery as RS data for monitoring bodies of water and found it to be very effective

Satellite images provide a synoptic perspective of vast areas, regular observations, and historical archives that may be used to evaluate the large inundated areas and their influence on infrastructure, human, economic, and environmental factors. With the advancement of geographic information systems (GIS), spatial object data on the earth's surface is quickly provided and spatially analyzed. Therefore, mitigation efforts need to be undertaken to prevent risks that have the potential to become disasters or reduce the effects of disasters when it occurs (Faizana et al., 2015).

The novelty or research gap of this research is with a multi-index approach provides a more comprehensive and accurate assessment of flood risk. The use of Sentinel-2A images in this study is also a novel approach to flood risk assessment, as previous studies have primarily relied on traditional data sources such as topographic and rainfall data. The provision of geospatial data on the flooding potential in this study was used to achieve the Sustainable Development Goals (SDGs), which require the coordination between national, provincial, and district/city planning initiatives. The goal mainly relies on the pillars of environmental development, which include clean water and sanitary conditions, livable towns and cities, responsible consumption and production, managing climate change, and maintaining marine and terrestrial ecosystems are some examples.

## METHODS

### STUDY AREA

The study location is the Mempawah watershed in the province of West Kalimantan, and its sub-districts are part of the Landak and Mempawah districts. Figure 1 displays the study location.

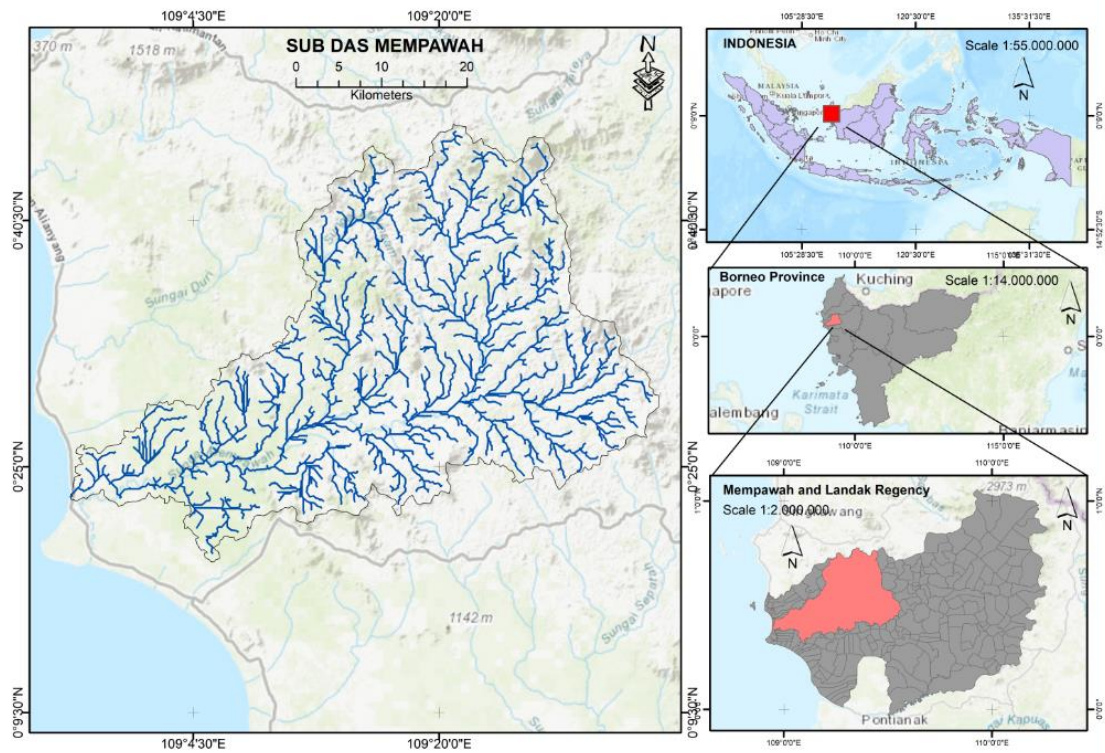


Figure 1. Study Area

### DATA ANALYSIS

The utilized method is an analysis of secondary data and survey from topographic maps, Sentinel 2A imagery that has been radiometrically and geometrically corrected using ArcGIS, DEM images, and 10 x 10 m resolution, acquired on 17 August 2019 and 21 November 2019 from the United State Geological Survey (USGS). Also, the secondary data analysis employed includes the Standardized Precipitation Index (SPI), Normalized Difference Vegetation Index (NDVI), Normalized Difference Water Index (NDWI), Soil Adjusted Vegetation Index (SAVI), and Inverse Distance Weighted (IDW). The ArcGIS 10.8 was used to explore data, while the methodology stages are shown in Figure 2.

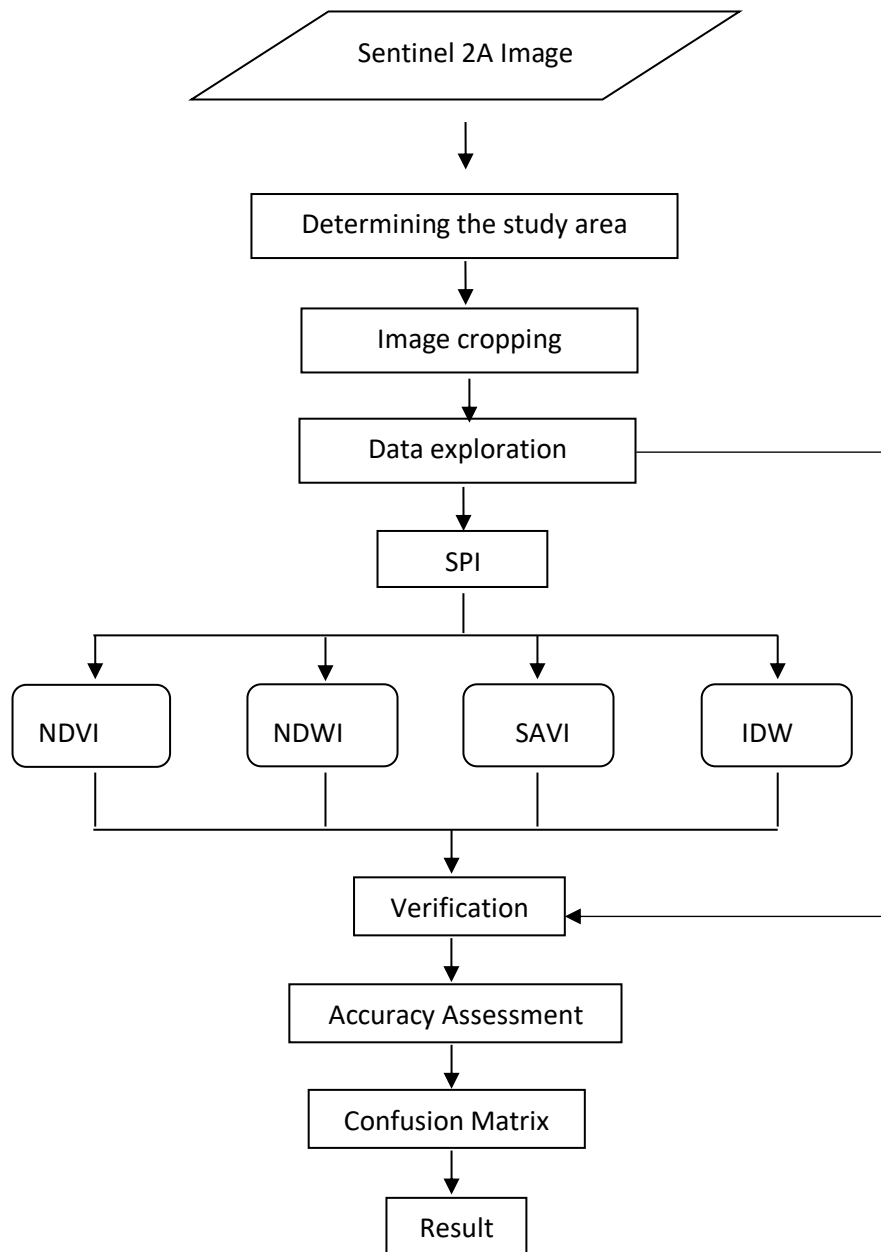


Figure 2. Research Flowchart

**Normalized Difference Vegetation Index (NDVI)**

The NDVI is a standard method for determining and comparing the greenness of plants i.e., chlorophyll content. The standard formula for calculating the NDIV value is as follows:

$$NDVI = \frac{NIR - RED}{NIR + RED} \tag{1}$$

Where:

NIR = Near-Infrared Band

RED = Red Band

Vegetation’s greenery level below 0.2 indicates that the place is already outside the vegetation group i.e., the body of water site or soil and rocks. Meanwhile, those above 0.4 have high vegetation values or heavy forest areas (Ginting & Jadera, 2018).

**Normalized Difference Water Index (NDWI)**

When analyzing the *Normalized Difference Water Index (NDWI)* with sentinel imagery, the bands utilized were 4 and 5. The first band was included in the near-infrared (NIR) spectral with a wavelength of 0.76 - 0.90 and was capable of distinguishing the vegetation type or plants detected for it to be limited and differentiated by water bodies and soil moisture. Meanwhile, band 5 with a wavelength of 1551.75 was included in the middle infrared and it helps to display vegetation and soil moisture, and also distinguishes between snow and clouds. This wetness index is called the normalized difference water index (NDWI), which is used to show bodies of water from satellite imagery. The NDWI formula is as follows:

$$NDWI = \frac{NIR - SWIR}{NIR + SWIR} \tag{2}$$

Where: NIR = Green Band

SWIR = Near Infra-Red Band

Table 1. NDWI Classification

Class	NDWI Value	Wetness Level
1	-1 < NDWI < 0	Non-Water Bodies
2	0 < NDWI < 0.33	Moderate Wetness
3	0.33 < NDWI < 1	High Wetness

Source: (Haikal, 2014)

**Soil Adjusted Vegetation Index (SAVI)**

The SAVI is known as the soil vegetation index or the Soil Adjusted Vegetation Index. This index is similar to the NDVI, but emphasizes the soil pixel effect using the crop canopy adjustment factor. The excellent index is primarily used in areas with relatively sparse vegetation where the soil is visible through the canopy (Sinaga et al., 2018).

$$SAVI = 1,5 * \frac{(NIR - Red)}{NIR + 0.5} \tag{3}$$

Where

NIR: Near Infra-Red Band (Band 5)

RED: Red Band (Band 4)

Table 2. SAVI Value Classification

Class	Density	Type of GOS
-0.3667 - 0.0187	Non-Green Open Space (GOS)	Body of water like a river
0.0187 - 0.1041	Very low	Open land settlements covered with asphalt or paving or asphalt roads
0.1041 - 0.3667	Low	Land cover vegetation, such as on dirt roads, empty fields without asphalt or paving
0.3667 - 0.5214	Moderate	Covered vegetation areas in the form of coconut plantations, mixed gardens of grass vegetation, golf courses, reeds
0.521 - 0.7895	High	Forest Vegetation

Source: (Laurensz et al., 2019)

### Standardized Precipitation Index (SPI)

The SPI is an index of deviations from the average rainfall over a long period, such as one month, two, or three. Furthermore, the method was developed in 1993 by McKee for measuring the rainfall deficit based on its normal conditions at different periods. The classification in the SPI was for determining the drought intensity and the incidence of deficiency at a specific time. It was discovered that continuous weakness was detrimental, reaching drought intensity with an SPI of -1 or less, and ends when the value becomes positive (McKee et al., 1993; Saidah et al., 2017).

Table 3. SPI Value Classification

SPI Value	Classification
$\geq 2.00$	Extremely Wet
1.50 - 1.99	Very wet
1.00 - 1.49	Wet Enough
-0.99 - 0.99	Close to Normal
-1.00 - -1.99	Dry Enough
-1.5 - -1.99	Very Dry
$\leq -2.00$	Extremely Dry

Source: (McKee et al., 1993; Saidah et al., 2017)

### Inverse Distance Weighted (IDW)

This technique presupposes each entry point has a diminishing local effect on distance, which was interpolated and searched by mathematical formulas. In addition, the interpolation was relatively affected by the sample points and its power determines the effect on the inputs, which were more significant at the output when producing a more detailed surface (Pasaribu & Haryani, 2012). The potential flooding level in this current study was determined by overlaying the factors causing floods using ArcGIS with Weighted Overlay analysis. Table 4 shows the three classifications of the overlay results:

Table 4. Classification of Potential Flood Levels in the study area

Flood Potential Level	Description
High	Areas that are potentially prone to flooding and have an impact on community life,
Medium	Areas with no/less flooding and no/less impact on community life.
Low	The area has never experienced flooding and did not cause disaster.

### Confusion Matrix

The confusion matrix is the number of samples obtained from field verification and validation tests, expressed in a matrix containing columns and rows. Furthermore, the columns describe the field reference data while rows contain the classification results from processing. The respective class accuracy was obtained from the confusion matrix calculation by considering the inclusion and exclusion errors from the classification (Congalton & Green, 2019). It is significant to remember that the number of samples utilized in this research was 36.

**RESULTS AND DISCUSSION**

**Normalized Difference Vegetation Index (NDVI)**

According to the results of the Normalized Difference Vegetation Index (NDVI) analysis, the Mempawah watershed has a value range of -0.48 – 1. This value was classified into rare, moderate, and dense. Table 5 shows the area of each class. Based on the results, 70.37% of the plants in the Mempawah watershed are still dense. The results of the NDVI classification are seen in Figure 3.

Table 5. Density Class Area

Class	Large (Ha)	Percentage
Non-Vegetation	864,581	5.14
Rare vegetation	1,511,967	8.99
Medium vegetation	2,606,778	15.50
dense vegetation	11,834,453	70.37
Total	16,817,779	100.00

Another crucial flooding-related influencing element is the NDVI. The negative values show water and the positive values show vegetation so, NDVI has a negative relationship with flooding: higher NDVI values indicate a lower probability of flood and lower NDVI values indicate a higher flood probability as in the research (Khosravi et al., 2016; Paul et al., 2019; Ullah & Zhang, 2020).

Higher values indicate more vegetation and healthier vegetation. NDVI can indirectly affect the occurrence and severity of flood disasters in a number of ways. Healthy vegetation can absorb and store large amounts of water, reducing runoff and flooding. Conversely, areas with low vegetation cover or damaged vegetation are more likely to experience flooding because the soil cannot retain as much water. NDVI can also be used to track alterations in vegetation cover over time, which can help identify areas that are at greater risk of flooding due to deforestation or other land use changes.

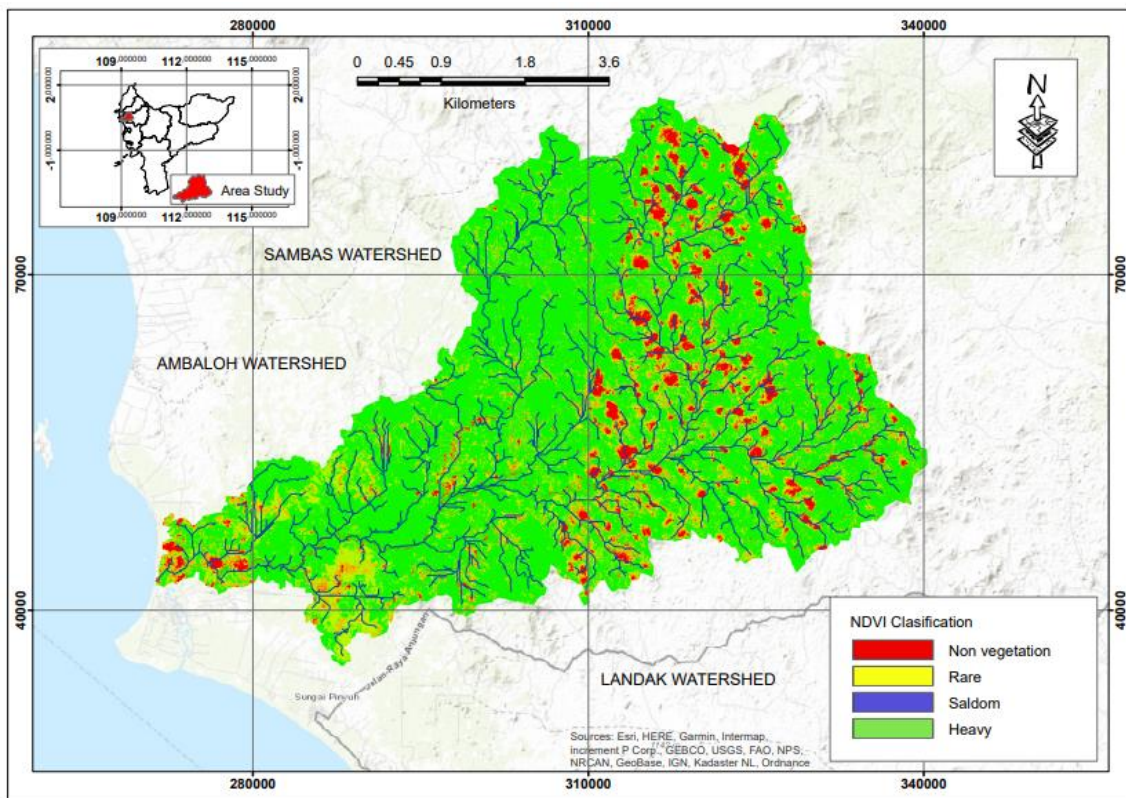


Figure 3. Normalized Difference Vegetation Index (NDVI)

### Normalized Difference Water Index (NDWI)

The NDWI in Mempawah watershed shows that non-water bodies have the most significant area of 11,991,529 ha indicating 71.30 %, with a value of  $-1 < 0$ . Furthermore, the moderate wetness area was 3,103,201 ha, representing 18.45 % with  $0 < 0.33$ , while the high wetness has an area of 172,3049 ha, denoting 10.25 %. Figure 4 shows the Normalized Difference Water Index (NDWI) in the Mempawah Watershed.

NDWI can be used to assess the potential risk of flooding in an area, as areas with higher NDWI values may be more susceptible to flooding due to the presence of surface water or saturated soils. NDWI can also be used to monitor changes in water levels over time, which can help predict and prepare for potential flood events (Farhadi & Najafzadeh, 2021; Sajjad et al., 2023; Sivanpillai et al., 2021 ). From Figure 4, most water areas are in the eastern part of the watershed, while those around the river are in the west.

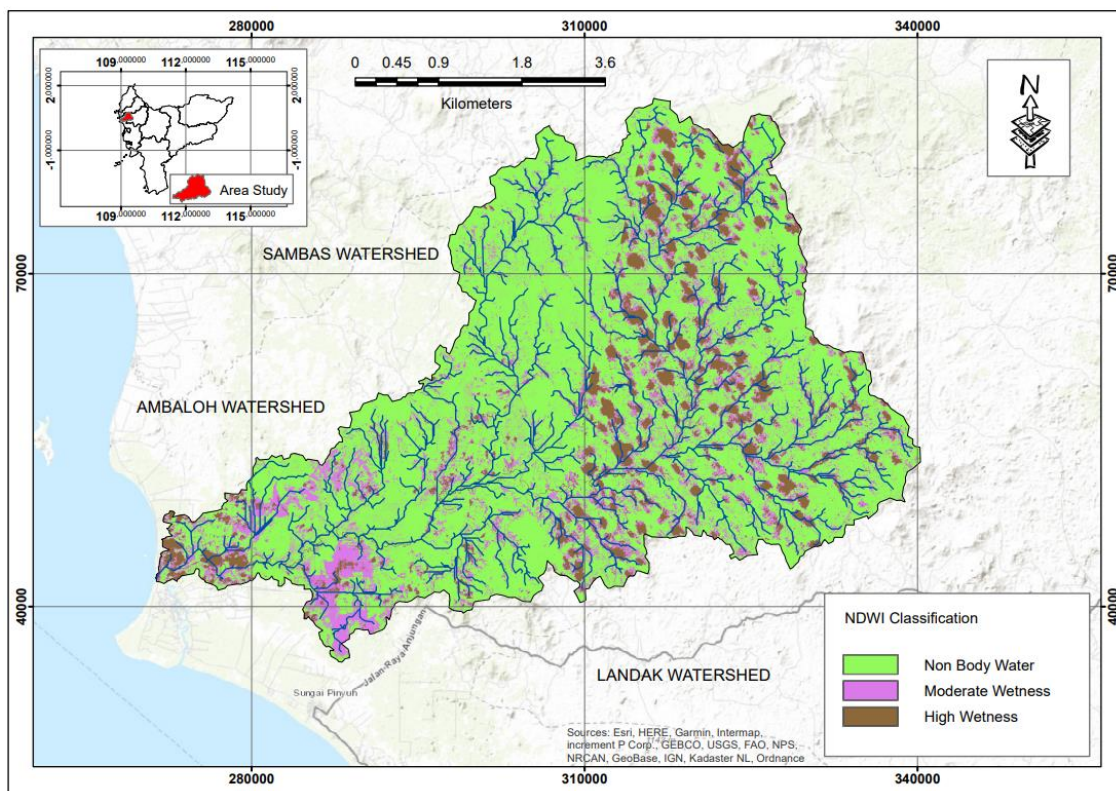


Figure 4. Normalized Difference Water Index (NDWI)

### Soil Adjusted Vegetation Index (SAVI)

The Soil Adjusted Vegetation Index (SAVI) is at a high class, which shows that most Mepawah watershed areas are Green Open Space (GOS) in the form of forest vegetation. Based on the ArcGIS analysis, the GOS of the Mempawah watershed has an area of 15,579,069 ha, representing 92.63 %, as shown in Figure 5.

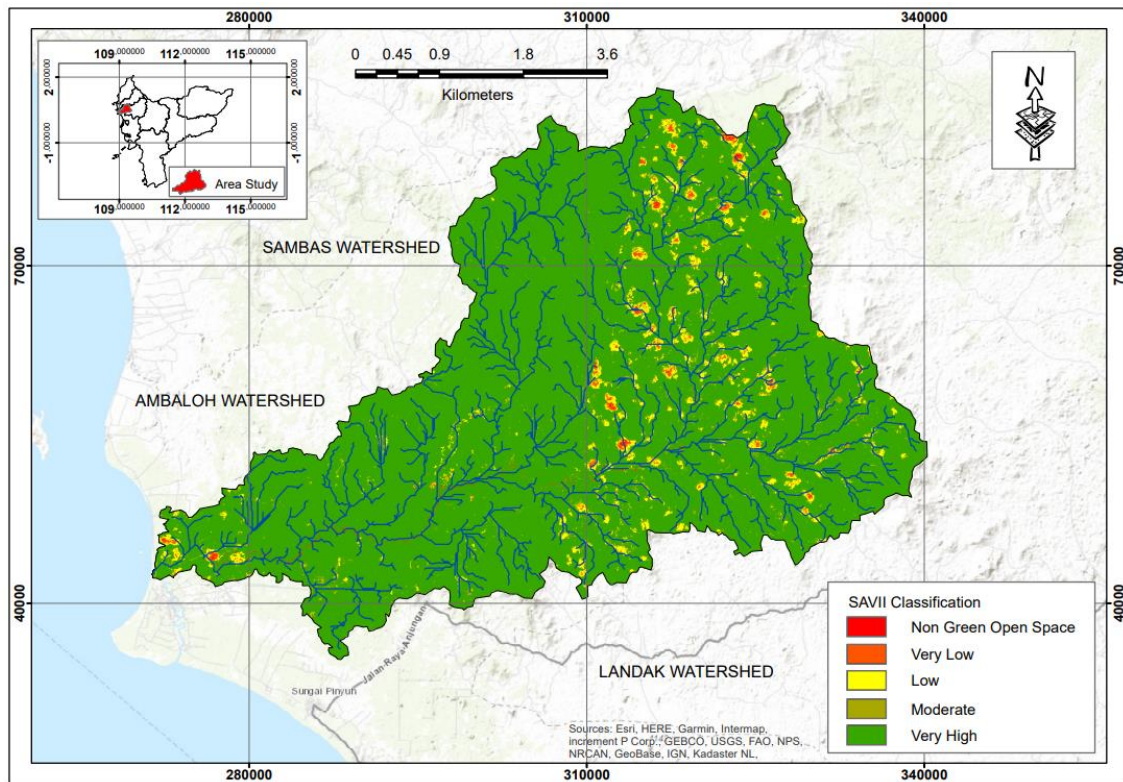


Figure 5. Soil Adjusted Vegetation Index (SAVI)

From Figure 5, the high SAVI index has a value of 0.521 – 0.7895, which means that the canopy density in the Mempawah watershed was also relatively high. It was observed that when the SAVI index increased, the vegetation canopy in the area was denser. In the context of flood disasters, high SAVI values can indicate that an area has a dense vegetation cover that can help to mitigate the effects of flooding. Vegetation helps to absorb and slow down the movement of water, reducing the likelihood of flash floods and soil erosion. In addition, vegetation can help to stabilize soil, preventing landslides and other forms of soil instability (Rhyma et al., 2020).

#### Standardized Precipitation Index (SPI)

The Standardized Precipitation Index (SPI) value ranges from 1.14 to 2.00. Furthermore, the SPI index shows a positive value, indicating that the Mepawah watershed condition was wet. According to Saidah (2017), the SPI index of the Mempawah watershed showed a moderately moist to very damp class. A positive SPI value also indicates above-average rainfall due to the SPI's normalization. Humid and dry climates were depicted in a similar manner, which means the damp period was also monitored with SPI. The SPI index of the Mempawah watershed is seen in Figure 6.

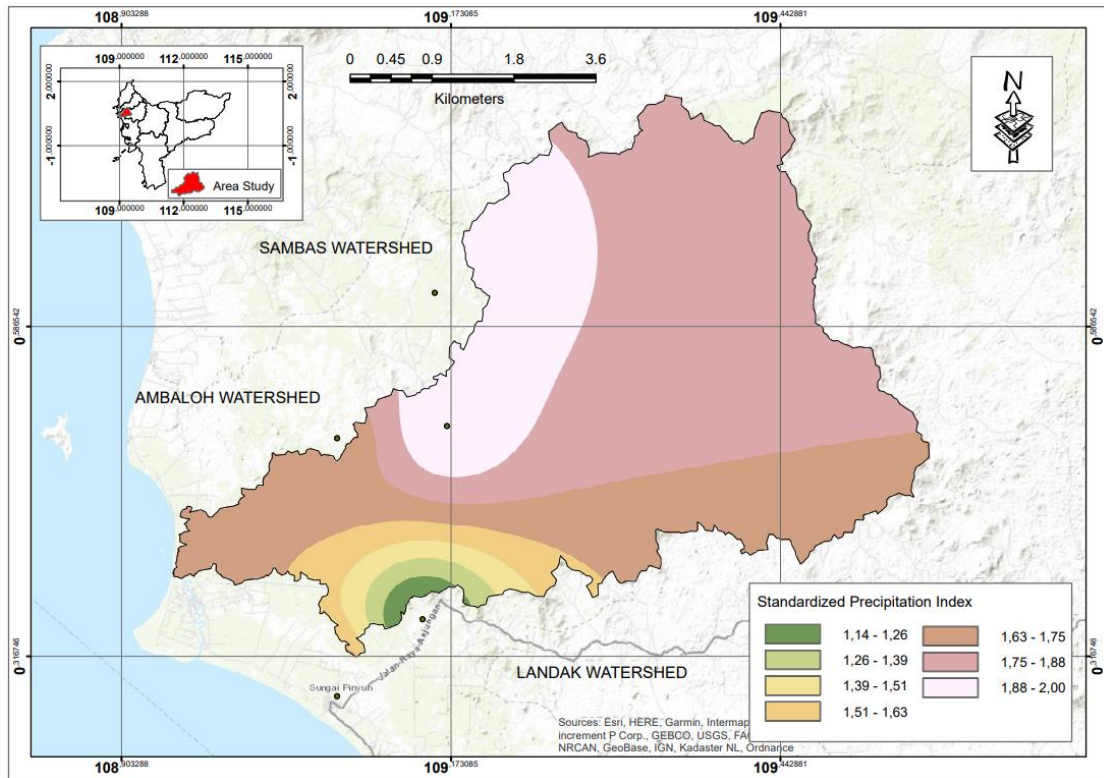


Figure 6. Standardized Precipitation Index (SPI)

It was discovered that areas with a very wet SPI index are wider than those that are moderately moist. The sites with a very wet value are distributed in the north and west of the sub-watershed area. In the context of flood disasters, high SPI values can indicate that an area is at a higher flooding danger because of the increased amount of rainfall or snowmelt. When the SPI value is high, it means that the amount of precipitation received in the area is more than what is typically expected, which can lead to increased water levels in rivers, lakes, and other water bodies, increasing the risk of flooding (Nguyen-Huy et al., 2022).

### Inverse Distance Weighted (IDW)

Inverse Distance Weighted (IDW) uses several weights for searching radius, namely variable and fixed search radius. The weighting was based on the influence of 1 to 5, while only the positive value was employed for selecting the difference.

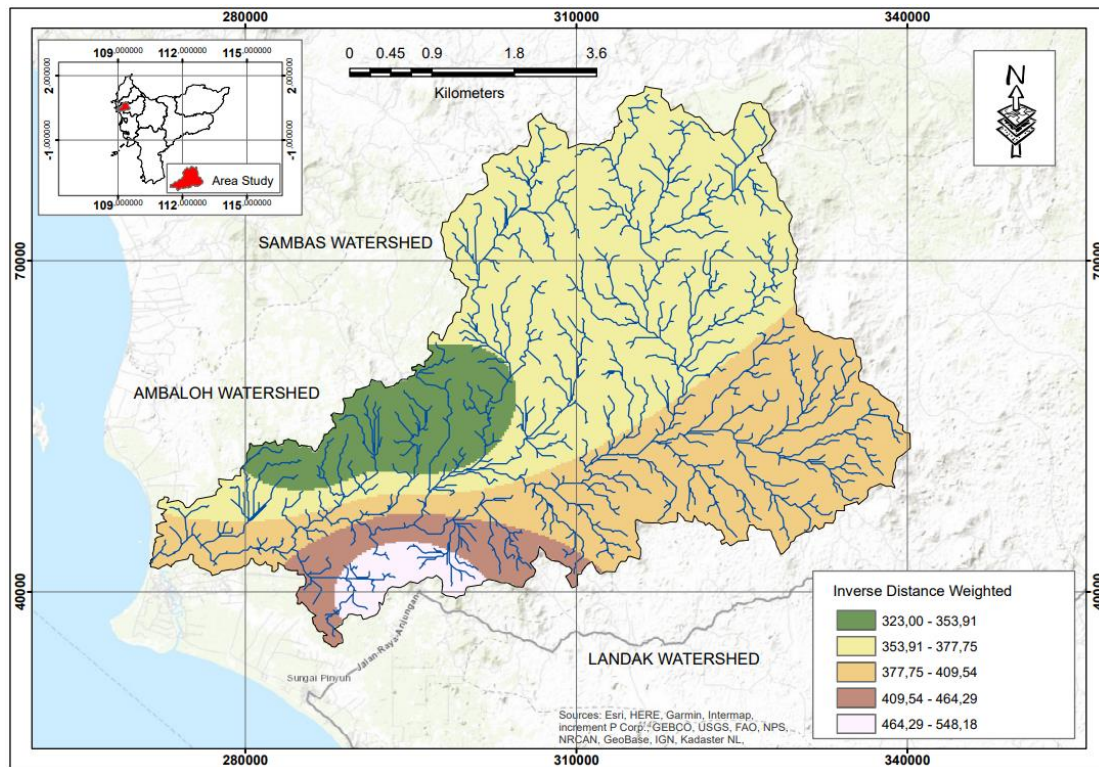


Figure 7. Inverse Distance Weighted (IDW)

The interpretation of data processing using ArcGis 8 showed that the IDW value varies. For example, when the power generated was high, the result was more concentrated with low attention. This means that the IDW was influenced by the area affecting the interpolated point. It was observed that flood occurrences in the Mempawah watershed have changed due to the wider area that originally had low to medium flood potential and from low to high. The potential for past mid and high-level flooding in this location has been relatively low, but now becoming more widespread. [Figure 8](#) shows the past flood occurrences in Mempawah watershed.

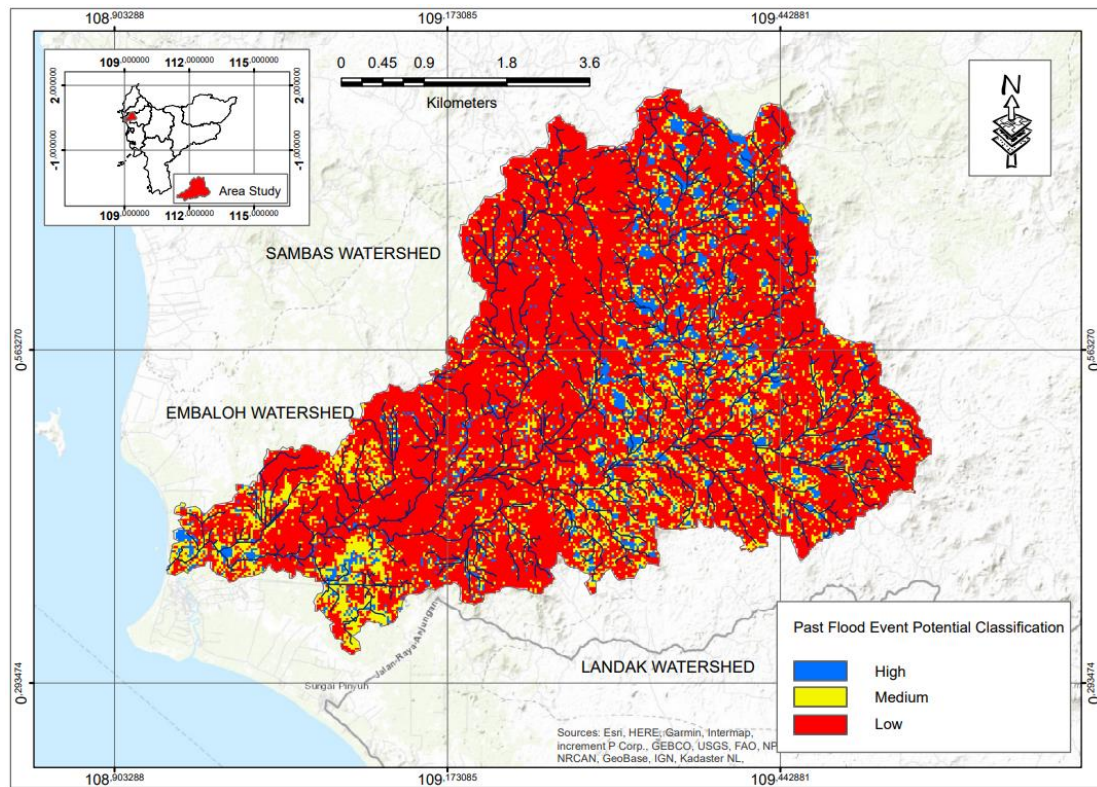


Figure 8. Past Floods Occurrence Potential at Mempawah Watershed

The recent analytical results of the flooding potential in the Mempawah Watershed are shown in Figure 9. The potential for flooding was classified into three, namely high, medium, and low. It was observed that sites with high flood potential are mainly located at watersheds and partially along riverbanks. Places with high flood potential have an area of 1,511,967 ha, while those that are medium was 2,606,778 ha, and the ones having low value were 12,644,034 ha. The places that experienced changes during flooding from the initial to the present were shown in Table 6. This occurrence of change showed variations in levels from; 1) low to medium, 2) medium to high, and 3) low to high.

The distance from one river to another is measured by the soil vegetation index or the Soil Adjusted Vegetation Index (SAVI). It was observed that places with a high potential for flooding have a low NDVI value, indicating that many lands are exposed due to a lack of vegetation. Meanwhile, when the wetness of the place or water body was wide, there was an increase in the NDWI value. In addition, high rainfall causes seawater to be tidal and inundate land areas since it is close to the sea.

Places with vegetation often have moderate flood potential as observed from the average NDVI values. Similarly, both the NDWI and SAVI showed a moderate value because the vegetation is no longer dense. The distance between the rivers is relatively small, therefore when it drains, the water quickly concentrates at one point. However, this place is far from the influence of seawater in the event of a tidal flood.

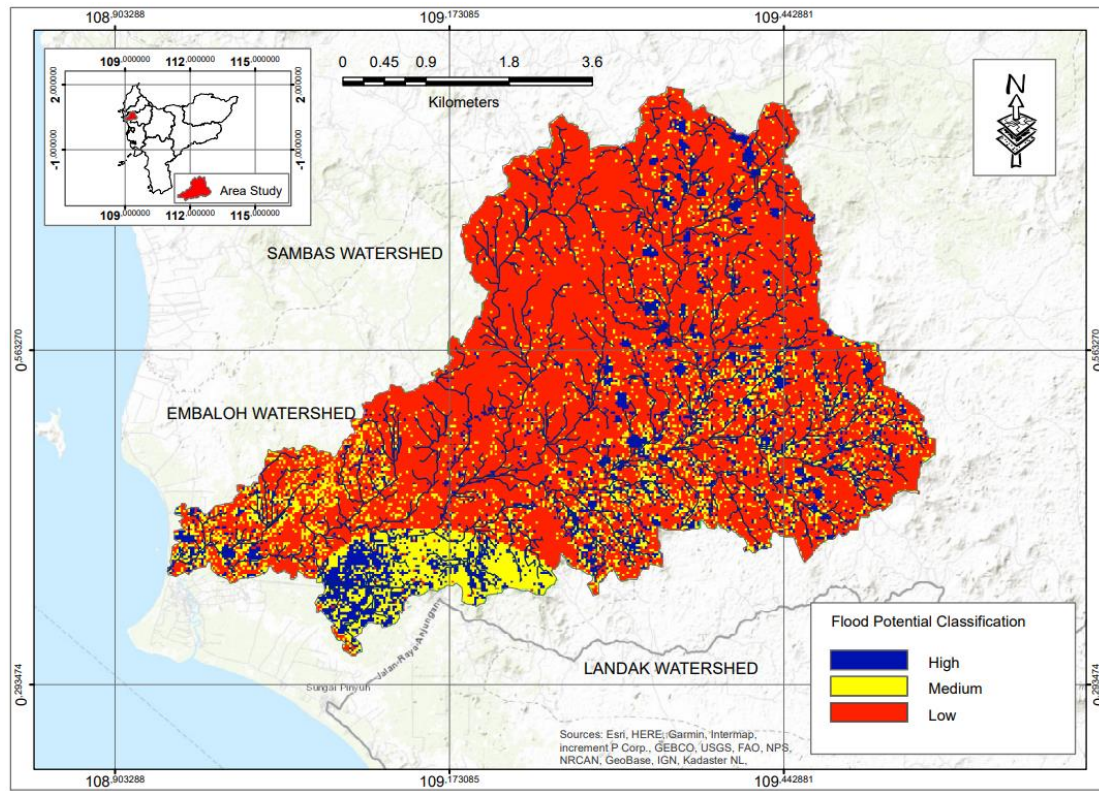


Figure 9. The Latest Potential Flood Occurrence at the Mempawah Watershed

Furthermore, places having low flood potential are due to the high Normalized Difference Vegetation Index (NDVI) region. The vegetation in this location was still dense, hence the rainwater on the surface was absorbed into the ground, which reduces surface runoff. It was observed that the NDWI and wetness values were respectively low, due to the absence of water bodies, but the SAVI was high because the place still has dense vegetation and forest. In addition, the distance between rivers was far and the location has a rough topography in the upstream region.

Field verification conducted visually aims to compare the processing results of GIS with actual field conditions, in order to be assured that the analytical output is correct. Table 6 shows the places experiencing changes in flood events.

Table 6. Flood Changes verification in Mempawah Sub-Watershed

No	Coordinate (Lat;Long)	Village	Flood Change
1	109,206:0.388	Kecurit	Low to Medium
2.	109,144:0.402	Terap	Low to Medium
3	109,095:0.393	Anjungan Dalam	Medium to High
4.	109,075:0.355	Anjungan	Medium to High
5.	109,083:0.341	Besar Laut	Low to High
6	108,948:0.391	Terusan	Medium to High
7	109,129:0.367	Anjungan Selancar	Low to High

After conducting field verification, an accuracy test was performed using a confusion matrix. Table 7 shows the field verification results of the confusion matrix.

Table 7. Field Verification using Confusion Matrix

	V/P	Processing		
		Change	No change	Total
Verification	Change	20	2	22
	No Change	4	10	14
	Total	24	12	36

Tabel 8. User's Accuracy and Producer's Accuracy

Classification	User's Accuracy (%)	Producer's Accuracy (%)
Change	90.909	83.333
No Change	71.428	83.333

The user's accuracy in Table 8 is the number of correct samples divided by the total samples. Furthermore, it was employed to determine the accuracy level based on image interpretation results. The changes in the results of class users' accuracy reached 90.909%, while those that did not change were 83.333%. A satellite evaluation rate of > 70% was described as good (Gallego et al., 2014; Rivas-Fandiño et al., 2023). This means that when the accuracy of the interpretation results and change detection approach was good, the producer's accuracy in each class was also good with a value > 88.333%.

## CONCLUSION

The GIS approach and the remote sensing data are effective tools for mapping potential floods. Furthermore, the GIS and remote sensing-based flood potential mapping are valuable tools for estimating flood-prone places, as well as helping water resource planners and decision-makers should concentrate on particular regions when performing a more detailed flood assessment. With remote sensing and geographic information systems as instruments for estimating and predicting floods, future occurrences are preventable. This is because the system is capable of predicting places prone to flood, thereby reducing property damage and even loss of lives. Geospatial information obtained from Sentinel 2A imagery, supported by a GIS was quickly deployed and spatially analyzed. Therefore, mitigation efforts need to be undertaken when managing the risks that potentially become disasters or reducing their impact when it occurs. From the facts above, the usage of Remote Sensing data and GIS has to be increased in order to support disaster management, particularly flooding.

## ACKNOWLEDGMENTS

The authors would like to thank Land Rehabilitation, and Soil Conservation (Forestry Service), and Disaster Management Service West Kalimantan Province has provided the research facilities.

## DECLARATIONS

### Conflict of Interest

The authors declare that in the research and preparation of this article, there are no conflict of interests related to certain organizations, institutions, and individuals or groups.

### **Ethical Approval**

On behalf of all authors, the corresponding author states that the paper satisfies Ethical Standards conditions, no human participants, or animals are involved in the research.

### **Informed Consent**

On behalf of all authors, the corresponding author states that no human participants are involved in the research and, therefore, informed consent is not required by them.

### **DATA AVAILABILITY**

Data used to support the findings of this study are available from the corresponding author upon request.

### **REFERENCES**

- Abdelkarim, A., Gaber, A. F. D., Alkadi, I. I., & Alogayell, H. M. (2019). Integrating remote sensing and hydrologic modeling to assess the impact of land-use changes on the Increase of flood risk: A Case study of the Riyadh–Dammam Train Track, Saudi Arabia. *Sustainability*, 11(21), 6003. <https://doi.org/10.3390/su11216003>.
- Abdelkarim, A., Gaber, A. F. D., Youssef, A. M., & Pradhan, B. (2019). Flood hazard assessment of the urban area of Tabuk City, Kingdom of Saudi Arabia by integrating spatial-based hydrologic and hydrodynamic modeling. *Sensors*, 19(5), 1024. <https://doi.org/10.3390/s19051024>.
- Ali, S. A., Parvin, F., Pham, Q. B., Vojtek, M., Vojteková, J., Costache, R., Linh, N. T. T., Nguyen, H. Q., Ahmad, A., & Ghorbani, M. A. (2020). GIS-based comparative assessment of flood susceptibility mapping using hybrid multi-criteria decision-making approach, naïve Bayes tree, bivariate statistics and logistic regression: A case of Topľa basin, Slovakia. *Ecological Indicators*, 117, 106620. <https://doi.org/10.1016/j.ecolind.2020.106620>.
- Brath, A., Montanari, A., & Moretti, G. (2006). Assessing the effect on flood frequency of land use change via hydrological simulation (with uncertainty). *Journal of Hydrology*, 324(1–4), 141–153.
- Caballero, I., Ruiz, J., & Navarro, G. (2019). Sentinel-2 satellites provide near-real time evaluation of catastrophic floods in the West Mediterranean. *Water (Switzerland)*, 11(12). <https://doi.org/10.3390/w11122499>
- Caruso, G. D. (2017). The legacy of natural disasters: The intergenerational impact of 100 years of disasters in Latin America. *Journal of Development Economics*, 127, 209–233. <https://doi.org/10.1016/j.jdeveco.2017.03.007>.
- Congalton, R. G., & Green, K. (2019). *Assessing the accuracy of remotely sensed data: principles and practices*. CRC press.
- Curebal, I., Efe, R., Ozdemir, H., Soykan, A., & Sönmez, S. (2016). GIS-based approach for flood analysis: case study of Keçidere flash flood event (Turkey). *Geocarto International*, 31(4), 355–366. <https://doi.org/10.1080/10106049.2015.1047411>.
- Dano, U. L., Balogun, A.-L., Matori, A.-N., Wan Yusouf, K., Abubakar, I. R., Said Mohamed, M. A., Aina, Y. A., & Pradhan, B. (2019). Flood susceptibility mapping using GIS-based analytic network process: A case study of Perlis, Malaysia. *Water*, 11(3), 615. <https://doi.org/10.3390/w11030615>.

- Diakakis, M., Deligiannakis, G., Antoniadis, Z., Melaki, M., & ... (2020). Proposal of a flash flood impact severity scale for the classification and mapping of flash flood impacts. *Journal of Hydrology*, 590, 125452. <https://doi.org/10.1016/j.jhydrol.2020.125452>.
- Faizana, F., Nugraha, A. L., & Yuwono, B. D. (2015). Pemetaan risiko bencana tanah longsor Kota Semarang. *Jurnal Geodesi Undip*, 4(1), 223–234.
- Farhadi, H., & Najafzadeh, M. (2021). Flood risk mapping by remote sensing data and random forest technique. *Water*, 13(21). <https://www.mdpi.com/2073-4441/13/21/3115>.
- Fernández, D. S., & Lutz, M. A. (2010). Urban flood hazard zoning in Tucumán Province, Argentina, using GIS and multicriteria decision analysis. *Engineering Geology*, 111(1–4), 90–98.
- Gallego, F. J., Kussul, N., Skakun, S., Kravchenko, O., Shelestov, A., & Kussul, O. (2014). Efficiency assessment of using satellite data for crop area estimation in Ukraine. *International Journal of Applied Earth Observation and Geoinformation*, 29, 22–30. <https://doi.org/10.1016/j.jag.2013.12.013>.
- Ginting, J. A., & Jadera, A. M. (2018). Analisa indeks vegetasi menggunakan citra satelit Lansat 7 dan Lansat 8 menggunakan metode K-Means di Kawasan Gunung Sinabung. *Indonesian Journal of Computing and Modeling*, 1(1), 42–48.
- Haikal, T. (2014). Analisis Normalized Difference Wetness Index (NDWI) Dengan Menggunakan Data Citra Landsat 5 Tm (Studi Kasus: Provinsi Jambi Path/Row: 125/61). *Skripsi Fakultas Matematika Dan Ilmu Pengetahuan Alam Institut Pertanian Bogor*.
- Halmy, M. W. A., Gessler, P. E., Hicke, J. A., & Salem, B. B. (2015). Land use/land cover change detection and prediction in the north-western coastal desert of Egypt using Markov-CA. *Applied Geography*, 63, 101–112. <https://doi.org/10.1016/j.apgeog.2015.06.015>.
- Huong, H. T. L., & Pathirana, A. (2013). Urbanization and climate change impacts on future urban flooding in Can Tho city, Vietnam. *Hydrology and Earth System Sciences*, 17(1), 379. <https://doi.org/10.5194/hess-17-379-2013>.
- Khosravi, K., Nohani, E., Maroufinia, E., & Pourghasemi, H. R. (2016). A GIS-based flood susceptibility assessment and its mapping in Iran: a comparison between frequency ratio and weights-of-evidence bivariate statistical models with multi-criteria decision-making technique. *Natural Hazards*, 83, 947–987. <https://doi.org/10.1007/s11069-016-2357-2>.
- Komolafe, A. A., Awe, B. S., Olorunfemi, I. E., & Oguntunde, P. G. (2020). Modelling flood-prone area and vulnerability using integration of multi-criteria analysis and HAND model in the Ogun River Basin, Nigeria. *Hydrological Sciences Journal*, 65(10), 1766–1783. <https://doi.org/10.1080/02626667.2020.1764960>.
- Laurensz, B., Lawalata, F., & Prasetyo, S. Y. J. (2019). Potensi Resiko Banjir dengan Menggunakan Citra Satelit (Studi Kasus: Kota Manado, Provinsi Sulawesi Utara). *Indonesian Journal of Computing and Modeling*, 2(1), 17–24.
- Li, Y., Martinis, S., Plank, S., & Ludwig, R. (2018). An automatic change detection approach for rapid flood mapping in Sentinel-1 SAR data. *International journal of applied earth observation and geoinformation*, 73, 123-135. <https://doi.org/10.1016/j.jag.2018.05.023>.
- Mao, D., & Cherkauer, K. A. (2009). Impacts of land-use change on hydrologic responses in the Great Lakes region. *Journal of Hydrology*, 374(1–2), 71–82.

- McKee, T. B., Doesken, N. J., & Kleist, J. (1993). The relationship of drought frequency and duration to time scales. *Proceedings of the 8th Conference on Applied Climatology*, 17(22), 179–183.
- Muhari, A. (2021). *Sebanyak 674 Rumah di 5 Kecamatan Terdampak Banjir di Kabupaten Mempawah*. Plt. Kepala Pusat Data, Informasi Dan Komunikasi Kebencanaan BNPB. <https://bnpb.go.id/berita/Sebanyak-674-rumah-di-5-kecamatan-terdampak-banjir-di-kabupaten-mempawah>. Accessed April 18, 2023.
- Mukherjee, F., & Singh, D. (2020). Detecting flood prone areas in Harris County: A GIS based analysis. *GeoJournal*, 85(3), 647–663. <https://doi.org/10.1007/s10708-019-09984-2>.
- Munawar, H. S., Hammad, A. W. A., & Waller, S. T. (2022). Remote Sensing Methods for Flood Prediction: A Review. *Sensors*, 22(3). <https://doi.org/10.3390/s22030960>
- Nguyen-Huy, T., Kath, J., Nagler, T., Khaung, Y., Aung, T. S. S., Mushtaq, S., Marcussen, T., & Stone, R. (2022). A satellite-based Standardized Antecedent Precipitation Index (SAPI) for mapping extreme rainfall risk in Myanmar. *Remote Sensing Applications: Society and Environment*, 26, 100733. <https://doi.org/10.1016/j.rsase.2022.100733>.
- Ovando, A., Martinez, J. M., Tomasella, J., Rodriguez, D. A., & von Randow, C. (2018). Multi-temporal flood mapping and satellite altimetry used to evaluate the flood dynamics of the Bolivian Amazon wetlands. *International Journal of Applied Earth Observation and Geoinformation*, 69, 27-40. <https://doi.org/10.1016/j.jag.2018.02.013>.
- Pasaribu, J. M., & Haryani, N. S. (2012). Perbandingan Teknik Interpolasi DEM SRTM dengan Metode Inverse Distance Weighted (IDW), Natural Neighbor dan Spline (Comparison of DEM SRTM Interpolation Techniques Using Inverse Distance Weighted (IDW), Natural Neighbor and Spline Method). *Jurnal Penginderaan Jauh Dan Pengolahan Data Citra Digital*, 9(2).
- Paul, G. C., Saha, S., & Hembram, T. K. (2019). Application of the GIS-based probabilistic models for mapping the flood susceptibility in Bansloi sub-basin of Ganga-Bhagirathi river and their comparison. *Remote Sensing in Earth Systems Sciences*, 2, 120-146. <https://doi.org/10.1007/s41976-019-00018-6>.
- Purwanto, A., Rustam, R., Andrasromo, D., & Eviliyanto, E. (2022). Flood risk mapping using GIS and multi-criteria analysis at Nanga Pinoh West Kalimantan Area. *Indonesian Journal of Geography*, 54(3). <https://doi.org/10.22146/ijg.69879>.
- Rawat, J. S., Biswas, V., & Kumar, M. (2013). Changes in land use/cover using geospatial techniques: A case study of Ramnagar town area, district Nainital, Uttarakhand, India. *The Egyptian Journal of Remote Sensing and Space Science*, 16(1), 111–117. <https://doi.org/10.1016/j.ejrs.2013.04.00>.
- Rhyman, P. P., Norizah, K., Hamdan, O., Faridah-Hanum, I., & Zulfa, A. W. (2020). Integration of normalised different vegetation index and Soil-Adjusted Vegetation Index for mangrove vegetation delineation. *Remote Sensing Applications: Society and Environment*, 17, 100280. <https://doi.org/10.1016/j.rsase.2019.100280>.
- Rincón, D., Khan, U. T., & Armenakis, C. (2018). Flood risk mapping using GIS and multi-criteria analysis: A greater Toronto area case study. *Geosciences*, 8(8), 275. <https://doi.org/10.3390/geosciences8080275>.

- Rivas-Fandiño, P., Acuña-Alonso, C., Novo, A., Pacheco, F. A. L., & Álvarez, X. (2023). Assessment of high spatial resolution satellite imagery for monitoring riparian vegetation: riverine management in the smallholding. *Environmental Monitoring and Assessment*, 195(1), 81. <https://doi.org/10.1007/s10661-022-10667-8>.
- Saidah, H., Budianto, M. B., & Hanifah, L. (2017). Analisa indeks dan sebaran kekeringan menggunakan metode standardized precipitation index (SPI) dan geographical information system (GIS) Untuk Pulau Lombok. *Jurnal Spektran*, 5(2), 173–179.
- Sajjad, A., Lu, J., Chen, X., Chisenga, C., & Mazhar, N. (2023). Rapid assessment of riverine flood inundation in Chenab floodplain using remote sensing techniques. *Geoenvironmental Disasters*, 10(1), 1–18. <https://doi.org/10.1186/s40677-023-00236-7>.
- Saravi, S., Kalawsky, R., Joannou, D., Rivas Casado, M., Fu, G., & Meng, F. (2019). Use of artificial intelligence to improve resilience and preparedness against adverse flood events. *Water*, 11(5), 973. <https://doi.org/10.3390/w11050973>.
- Schnebele, E., & Cervone, G. (2013). Improving remote sensing flood assessment using volunteered geographical data. *Natural Hazards and Earth System Sciences*, 13(3), 669–677. <https://doi.org/10.5194/nhess-13-669-2013>.
- Shah, S. A., Seker, D. Z., Hameed, S., & Draheim, D. (2019). The rising role of big data analytics and IoT in disaster management: recent advances, taxonomy and prospects. *IEEE Access*, 7, 54595–54614. <https://doi.org/10.1109/ACCESS.2019.2913340>.
- Sheng, J., & Wilson, J. P. (2009). Watershed urbanization and changing flood behavior across the Los Angeles metropolitan region. *Natural Hazards*, 48(1), 41–57.
- Sholihah, Q., Kuncoro, W., Wahyuni, S., Suwandi, S. P., & Feditasari, E. D. (2020). The analysis of the causes of flood disasters and their impacts in the perspective of environmental law. *IOP Conference Series: Earth and Environmental Science*, 437(1), 12056. <https://doi.org/10.1088/1755-1315/437/1/012056>.
- Sinaga, S. H., Suprayogi, A., & Haniah, H. (2018). Analisis ketersediaan ruang terbuka hijau Dengan Metode Normalized Difference Vegetation Index dan Soil Adjusted Vegetation Index Menggunakan Citra Satelit Sentinel-2A (Studi Kasus: Kabupaten Demak). *Jurnal Geodesi Undip*, 7(1), 202–211.
- Sivanpillai, R., Jacobs, K. M., Mattilio, C. M., & Piskorski, E. V. (2021). Rapid flood inundation mapping by differencing water indices from pre-and post-flood Landsat images. *Frontiers of Earth Science*, 15, 1-11. <https://doi.org/10.1007/s11707-020-0818-0>.
- Skilodimou, H. D., Bathrellos, G. D., Chousianitis, K., Youssef, A. M., & Pradhan, B. (2019). Multi-hazard assessment modeling via multi-criteria analysis and GIS: a case study. *Environmental Earth Sciences*, 78(2), 47. <https://doi.org/10.1007/s12665-018-8003-4>.
- Tehrany, M. S., Pradhan, B., & Jebur, M. N. (2015). Flood susceptibility analysis and its verification using a novel ensemble support vector machine and frequency ratio method. *Stochastic Environmental Research and Risk Assessment*, 29, 1149–1165. <https://doi.org/10.1007/s00477-015-1021-9>.
- Ullah, K., & Zhang, J. (2020). GIS-based flood hazard mapping using relative frequency ratio method: A case study of Panjkora River Basin, eastern Hindu Kush, Pakistan. *Plos One*, 15(3), e0229153. <https://doi.org/10.1371/journal.pone.0229153>.

- Widiasari, I. R., & Nugroho, L. E. (2017). Deep learning multilayer perceptron (MLP) for flood prediction model using wireless sensor network based hydrology time series data mining. *2017 International Conference on Innovative and Creative Information Technology (ICITech)*, 1–5. [10.1109/INNOCIT.2017.8319150](https://doi.org/10.1109/INNOCIT.2017.8319150).
- Zhu, Z., & Woodcock, C. E. (2014). Continuous change detection and classification of land cover using all available Landsat data. *Remote Sensing of Environment*, 144, 152–171. <https://doi.org/10.1016/j.rse.2014.01.011>.